



Tool wear prediction model based on wear influence factor

Cheng Yang¹ · Yaoyao Shi¹ · Hongmin Xin^{1,2} · Tao Zhao¹ · Nan Zhang¹ · Chao Xian^{1,2}

Received: 21 February 2023 / Accepted: 6 September 2023 / Published online: 9 October 2023
© The Author(s), under exclusive licence to Springer-Verlag London Ltd., part of Springer Nature 2023

Abstract

This study proposed a new method for predicting tool wear curve over machining time through abscissa stretching or compressing based on wear influence factor, which is a tool wear prediction method with universal potential and relatively simple modeling and use. In this method, firstly, the relationship model between the tool wear rate and the cutting parameters needs to be built, and the wear influence factor can be derived from this relationship model. Then, it needs to record the curve of the tool wear value over machining time under a certain cutting parameters through experiments. This curve is called the benchmark tool wear curve, and the wear influence factor under these cutting parameters is called the benchmark wear influence factor. When the cutting parameters change, it is only required to solve the ratio between the wear influence factor under current cutting parameters and the benchmark wear influence factor, then use the ratio to stretch or compress the benchmark tool wear curve in the direction of the abscissa, that is the tool wear prediction curve under current cutting parameters. In this study, the tool wear curve under cutting parameter $V=55\text{m/min}$, $a_p=0.08\text{mm/tooth}$ is selected as the benchmark tool wear curve, and tool wear curves under cutting parameter $V=80\text{m/min}$, $a_p=0.12\text{mm/tooth}$, and $V=40\text{m/min}$, $a_p=0.06\text{mm/tooth}$ are accurately predicted. In the cross validation after the replacement of the benchmark tool wear curve, the prediction model also shows good prediction accuracy. The comprehensive optimization model of disc milling based on the wear influence factor shows that increasing the cutting line speed and reducing the feed per tooth can improve the cutting efficiency and reduce tool wear.

Keywords Tool wear · Model prediction · Influence factor · Scaling ratio

1 Introduction

During machining, it is necessary to maintain the sharpness of the cutting edge at all times, but in the actual cutting process, due to the coupling effect of cutting force, cutting temperature, cutting impact, cutting vibration and cutting friction, tool wear is unavoidable. Tool wear will greatly affect the cutting efficiency and the surface quality of parts. And if tool wears too fast, the blade needs to be replaced frequently, which not only prolongs the manufacturing cycle, but also increases the manufacturing cost. In addition, when

the machining accuracy requirements or machining types are different, the standard of tool bluntness will also change, so it is necessary to know when the tool wear value reaches the critical standard for tool change, which requires the ability to predict the tool wear. For these reasons, researching the mechanism of tool wear and predicting the process of tool wear has always been a hot research topic, which is also of great significance for optimizing cutting parameters and guiding the actual production. Many scholars have studied the mechanism and prediction of tool wear and accumulated a lot of related achievements.

There are many classic and famous achievements in the field of tool wear prediction models. Taylor [1] studied the relationship between cutting speed and tool durability in 1907 and proposed the famous tool durability formula. In Taylor's tool life formula, the exponential power of tool life multiplied by the cutting line speed is a constant. Archard [2] studied wear behavior based on contact friction theory and believed that increasing friction and load would exacerbate wear. Colding [3] proposed a tool life model with

✉ Hongmin Xin
xhm0330@163.com

¹ Key Laboratory of High Performance Manufacturing for Aero Engine (Northwestern Polytechnical University), Ministry of Industry and Information Technology, Xi'an 710072, China

² Hubei Key Laboratory of Power System Design and Test for Electrical Vehicle, Hubei University of Arts and Science, Xiangyang 441053, China

more parameters, which establishes the relationship between tool life, cutting speed, and equivalent chip thickness, taking into account other factors in the cutting process. These factors include tool material, tool shape, temperature, and workpiece processing performance. Using this model and its complex equations, the consequences of tool wear caused by simultaneous changes of multiple cutting conditions can be accurately calculated. Usui [4] proposed a tool wear prediction analysis method, which theoretically derived the tool wear characteristic equation. Only based on orthogonal cutting data and two wear characteristic parameters, it can realize the prediction of tool wear under various tool shapes and cutting conditions in turning. The predicted wear process and tool life are in good agreement with the experimental results.

Chetan [5] studied the wear mechanism of coated carbide tools when machining Ti6Al4V. The results showed that adhesive and diffusion wear are the dominating wear, and a tool wear model with cutting parameters as variables was formulated. In this model, the tool wear is positively correlated with cutting parameters which include cutting speed, feed rate and depth of cut. The experimental results show that the wear model can predict the flank wear under gentle cutting conditions. He [6] used 3D force analyzer and thermal imager to monitor the mechanical and thermal shock loads during machining, and studied the wear evolution process and wear mechanism of cemented carbide tools under thermal-mechanical coupling. Through statistical analysis, the cutting parameters corresponding to different wear modes are divided into regions, and the parameter region of safe cutting is obtained, which provides a method and theoretical reference for the selection of cutting parameters. Mao [7] believed that any point of wear on the cutting edge will degrade the overall cutting performance of the tool and reduce the surface integrity. On this basis, a tool wear prediction method considering local wear behavior was proposed. In this method, the wear rate of the cutting edge, the wear position, and the change in cutting length are considered, and the wear of cutting edge at each height is able to be predicted by the corresponding wear rate and cutting length. This method can be used to predict the value and position of the maximum wear on the tool flank. Aline [8] studied the tool wear behavior and mechanism in the micromachining, and believed that compared with the cutting process at the macro scale, the bluntness standard of cutting tools at the micro scale is different. With micro-tools, even a small wear zone can have a dramatic effect on the shear force at the entire cutting edge. On this basis, the experimental study of micromachining tool wear is carried out, and the Taylor's tool life equation for micromachining is obtained.

Luo [9] studied the relationship between tool flank wear and operating conditions during cutting with carbide inserts, and combined cutting mechanics simulation results with

empirical models to establish a tool flank wear rate model that can be used to predict the width of the tool flank wear. Experimental verification found that cutting speed has a greater impact on tool life than feed speed, and the predicted results are in good agreement with the measured results. Zhang [10] proposed a generalized wear model with adjustable coefficients, which considered the mechanism of the tool in different wear stages, and divided the entire tool life into three main wear areas according to the critical time, corresponding to the three main wear types: running-in wear, adhesive wear and three-body abrasive wear. The model is based on experimental data and refers to other well-known wear models to enhance adaptability and generalization. Based on this model, a method for predicting tool life was proposed and verified. Abhishek [11] developed a pseudo-analytic model of tool wear to predict wear behavior. The model comprehensively considered the hardness of the tool coating, workflow stress and the force acting on the tool, and realized the estimation of the tool wear value. The prediction model was verified by experiments, and the results demonstrated that the prediction model agrees well with the experimental results. Chinchankar [12] developed a flank wear rate model that considered wear, adhesion, and diffusion as the main wear mechanisms. The model only needs to determine the cutting conditions, the geometry of the tool, and the material parameters of the tool and workpiece, and it can predict the change of the flank wear value over machining time. The experimental results are consistent with the predicted data. Halila [13] developed a tool wear prediction model that considers contact sliding and sticking properties. This model is based on analytical methods, including statistical descriptions of particle distribution. In Halila's model, adhesive particles are assumed to be conical and embedded in the contact area. Halila believes that the sliding and sticking area at the tool-chip and tool-workpiece interfaces depend on the evolution of local stress conditions, sliding speed, and friction coefficient, and proposed a new abrasive wear model to estimate tool life. Laakso [14] proposed a new logit-function based model for wear rate, which can predict the tool wear at a given cutting speed, feed and at any given time within the tool life range, without selection the limiting tool wear. The prediction data are in good agreement with the experimental results. Zhang [15] proposed a physical model-based tool wear and damage monitoring method. Firstly, a physical model of milling force affected by tool runout and tool wear was established. Then, a tool wear monitoring method was proposed to extract comprehensive features from the seven channel specific cutting force coefficient by measuring milling force, spindle box vibration, and driving current. In addition, an effective tool breakage monitoring method has been proposed, which combines the amplitude ratio of multi-channel data to form indicators to determine the occurrence of tool breakage. Kamratowski

[16] studied a model of tool wear during gear machining. Firstly, the influence of process parameters and tool geometry on tool wear was analyzed using simulation software BeverCut, and a tool wear prediction model was established based on this. The algorithm of the model can be used to calculate the maximum chip thickness and solve it along the cutting edge of the blade in time and position. In addition, the model can also use the chip characteristics to determine the force required for elastic workpiece deformation. When establishing the wear prediction model, experimental and simulation results were combined to calibrate the model coefficients through multivariate regression analysis. Zhang [17] studied the tool wear model in milling using machining simulation methods, which can be used to predict the tool wear process during cutting. In this model, a tool wear model is established based on empirical tool wear data to estimate the tool wear value, based on this, the tool wear status is dynamically changing in the simulation software and can dynamically update the tool geometry structure. The experimental results verified the correctness of the tool wear simulation process based on the tool wear model.

There are also many scholars who have proposed prediction models of tool wear on the basis of various mathematical algorithms and optimization algorithms. LI [18] proposed a method for predicting the remaining tool life, which based on the tool wear mechanism and the Gaussian process regression model. In this model, based on the assumption of progressive tool wear process, the covariance matrix of the Gaussian model constrains the predicted value at adjacent moments to a linear relationship. In addition, in order to enhance the input feature space and output of the model, the tool wear mechanism is also considered to improve the prediction accuracy. Experimental results show that the proposed method can significantly improve the prediction of tool remaining service life. Wang [19] believed that the tool wear process and the milling process are very complex, and unpredictable disturbances made it difficult to accurately predict the tool wear value. Therefore, a Gaussian mixture regression model based on cutting force signal is proposed to realize the prediction of continuous tool wear. This model can improve the filtering effect on interference signals. Palanisamy [20] conducted cutting experiments with three factors and five levels. The experimental data were used to carry out tool wear prediction modeling through two methods. The first was to directly perform regression analysis modeling through experimental data. Another was to use experimental data to train a feed-forward back-propagation artificial neural network model. By comparing the errors between the two prediction models and the measured data, it was found that the prediction of the neural network model is more accurate. Mandal [21] selected machining conditions such as cutting speed, feed rate, and depth of cut as input, and modeled the flank wear in the cutting process

through the back-propagation neural network method. The result shows that the convergence of mean square error both in training and testing are excellent, and the accuracy of the prediction model was verified by experiments. Rao [22] proposed a method to estimate tool wear and roughness based on tool vibration when milling Ti-6Al-4V with carbide milling cutter. The grey prediction GM (1, N) system and support vector machine (SVM) were used respectively. The accuracy of the prediction model was verified through experiments. The result shows that the GM (1, N) optimization model had higher prediction accuracy. Zhang [23] established a tool wear prediction model based on the least squares support vector machine (LS-SVM) technology. In order to improve the accuracy of the model, the tool wear estimation results based on the LS-SVM model were updated by using the Kalman filter technique according to the measured tool wear values. The resulting model is called the LS-KF model and has higher accuracy. An [24] proposed a tool wear prediction model combining a convolutional neural network (CNN) with a stacked bi-directional and uni-directional LSTM (SBULSTM) network, called CNN-SBULSTM. In addition, a cyber-physical system (CPS) is also used in the model, which is used to collect internal controller signals and external sensor signals during milling. Li [25] proposed an integrated deep learning model for monitoring tool wear using audio sensors. Using audio denoising technology, combined with Fast Fourier Transform (FFT), bandpass filters, and Dependent Component Analysis (DCA), tool wear data during the cutting process was extracted. Then, train the integrated Convolutional Neural Network (CNN) detection model and use different algorithms to convert audio signals into audio images. The experimental results indicate that this method is very accurate in predicting tool wear values under different cutting conditions.

In summary, there have been many excellent researches on tool wear prediction, and many useful models have been obtained. However, many of them require a large number of training samples to improve the accuracy or are only suitable for specific machining process. In these models, in order to make the prediction results agree well with the experimental wear data, the modeling and optimization process are usually complicated and sensitive to machining conditions. If the machining system or conditions changed, some models may no longer be applicable. Thus, in order to solve these problems, a universal tool wear prediction method needs to be built.

The task of this study is to propose a tool wear prediction method, which can be used to predict the curve of tool wear value over machining time under different cutting parameters. The advantage of this tool wear prediction method is that it is not limited and constrained by the cutting type, cutting process and cutting conditions. As long as the model

of tool wear influence factor and the curve of tool wear value over machining time under a group of cutting parameters are obtained, the tool wear prediction model under any cutting parameters can be obtained by stretching or compressing the curve along the abscissa direction based on the wear influence factor. Therefore, it has the potential for universal applicability and is relatively simple to model and use.

2 Modeling method of tool wear prediction model based on wear influence factor

According to the basic tool wear theory [26], the wear process can be divided into three stages which include initial wear stage, steady wear stage and rapid wear stage, as shown in Fig. 1. In the initial wear stage, since the cutting edge is new, the tool wear rate is relatively high. After passing the initial wear stage, it begins to enter the steady wear stage, in which the tool wear rate slows down, the cutting system

is in a state of equilibrium and stability. When the tool wear reaches a certain value, the cutting edge is no longer sharp enough, as a consequence, more frictional heat is generated at the tool-chip interface, which leads to a dramatic acceleration of tool wear. This is the rapid wear stage, the cutting edge will become blunt in a short time.

Disc milling is a high-efficiency rough machining method for the aero-engine blisk [27] [28]. During the experimental research on disc milling tool wear without cooling, the phenomenon can be observed that if the machining equipment, cutting tool and workpiece remain unchanged, when different cutting parameters are used for machining, the curves of tool flank wear value over machining time are very similar in shape and trend, as shown in Fig. 2(a). The only obvious difference is that the wear speed is different. When the cutting parameters is $V=80\text{m/min}$, $a_p=0.06\text{mm/tooth}$, the tool wears quickly, while under cutting parameters $V=55\text{m/min}$, $a_p=0.04\text{mm/tooth}$, the tool wear rate is much slower, as shown in the comparison of VB_1 and VB_2 in Fig. 2(a).

Fig. 1 Three stages of the tool wear process

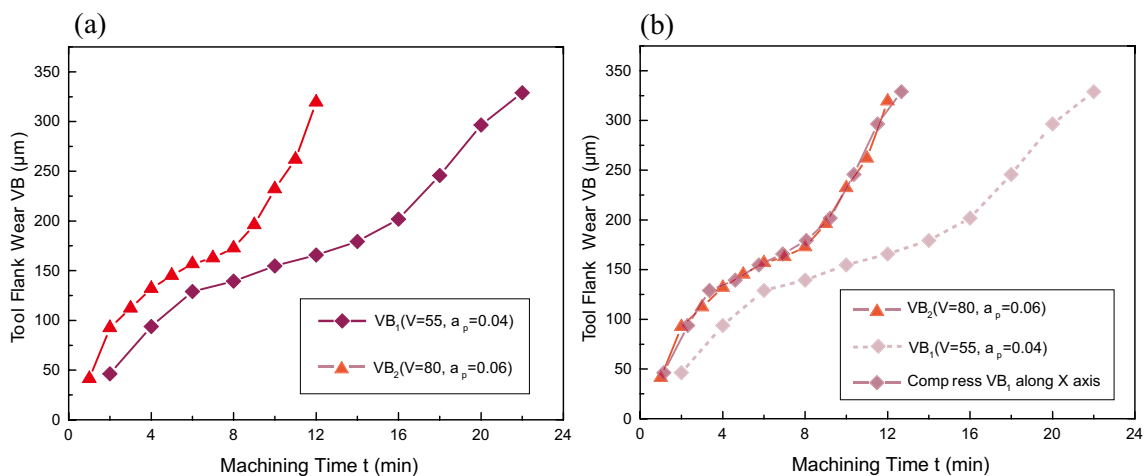
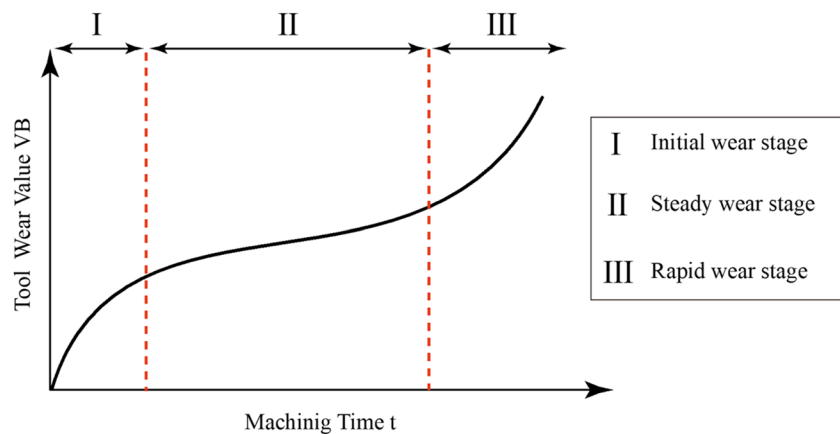


Fig. 2 Tool wear data of disc milling without cooling. (a) Comparison of VB_1 and VB_2 (b) comparison between VB_2 and VB_1 after abscissa compression

By compressing VB_1 along the X-axis, it is found that there is a high degree of coincidence with VB_2 under a suitable compressing ratio, as shown in Fig. 2(b), which provides a new possibility for the prediction of tool wear: whether as long as recording the tool wear curve under a set of cutting parameters, and stretch or compress this curve along the X-axis with a specific scaling ratio, so as to obtain the tool wear curve under another set of cutting parameters. This is the conjecture of tool wear prediction model with abscissa stretching or compressing proposed in this paper.

One of the most important unknowns in the prediction model conjecture is the scaling ratio for stretching or compressing. According to the analysis of the wear curve, the scaling ratio is determined by the ratio of the tool wear rate under two sets of cutting parameters. Therefore, the key to formulating the prediction model is to obtain a model that characterizes the relationship between tool wear rate and cutting parameters.

In this paper, a function $\eta(X)$ is introduced to characterize the relationship between tool wear rate and cutting parameters, which is called tool wear influence factor function, as shown in Eq. (1).

$$\eta(X) = g(x_1, x_2, \dots, x_n) \tag{1}$$

where $X = \{x_1, x_2, \dots, x_n\}$, which is a set consisting of various parameters that affect the tool wear rate during machining, each of x_1, x_2, \dots, x_n represents a different cutting parameter variable. When the value of any parameter in X changes, $\eta(X)$ will also change accordingly.

$\eta(X)$ can be obtained by modeling or regression analysis on the basis of tool wear experimental data under different cutting parameters, or obtained by finite element cutting simulation. In addition, an analytical theoretical model of $\eta(X)$ can also be established on the basis of the tool wear mechanism.

A function $VB(t)$ is introduced to represent the curve of tool wear value over machining time. According to the conjecture proposed in this paper, since $\eta(X)$ is a factor that characterizes the tool wear rate, when the value of $\eta(X)$ changes, the change reflected on the image of $VB(t)$ is that the abscissa of the curve will be compressed or stretched. The compressing or stretching of the abscissa is also equivalent to the shortening or lengthening of tool life. When the value of $\eta(X)$ increases, the abscissa will be compressed, otherwise the abscissa will be stretched. According to the mathematical properties of function abscissa stretching or compressing, the mathematical expression of compressing the abscissa by λ times is to multiply the independent variable by λ to form a new independent variable, as shown in Eq. (2).

$$y = f(x) \xrightarrow{\text{Compress the abscissa by } \lambda \text{ times}} y = f(\lambda x) \tag{2}$$

When the combination of cutting parameters is X_i , the wear influence factor is $\eta(X_i)$, if the tool wear curve $VB_i(t)$ under X_i has been obtained through the experimental data, when the combination of cutting parameters changes to X_j , the wear influence factor is $\eta(X_j)$, then the tool wear curve corresponding to X_j should be compressed by $\frac{\eta(X_j)}{\eta(X_i)}$ times on the basis of $VB_i(t)$, that is, replace the independent variable t with $\frac{\eta(X_i)}{\eta(X_j)}t$ and substitute it into $VB_i(t)$ to obtain the tool wear curve $VB_j(t)$ under X_j . As shown in Eq. (3).

$$\begin{cases} \eta(X) = g(x_1, x_2, \dots, x_n) \\ \lambda_{i,j} = \frac{\eta(X_j)}{\eta(X_i)} \\ VB_i(t) = f(t) \\ VB_j(t) = f(\lambda_{i,j}t) \end{cases} \tag{3}$$

where X_i is the i -th group of cutting parameters, X_j is the j -th group of cutting parameters, $\lambda_{i,j}$ is the scaling ratio for stretching or compressing. When $\lambda_{i,j} > 1$, $VB_j(t)$ is obtained by compressing the abscissa of $VB_i(t)$ by $\lambda_{i,j}$ times, and when $\lambda_{i,j} < 1$, $VB_j(t)$ is obtained by stretching the abscissa of $VB_i(t)$ by $1/\lambda_{i,j}$ times.

In the same way, if the tool wear prediction model with abscissa stretching or compressing proposed in this paper is correct, the tool life under different cutting parameters can also be directly calculated by wear influence factor. Assuming that the tool life under X_i is T_i , the tool life T_j under X_j can be calculated by Eq. (4).

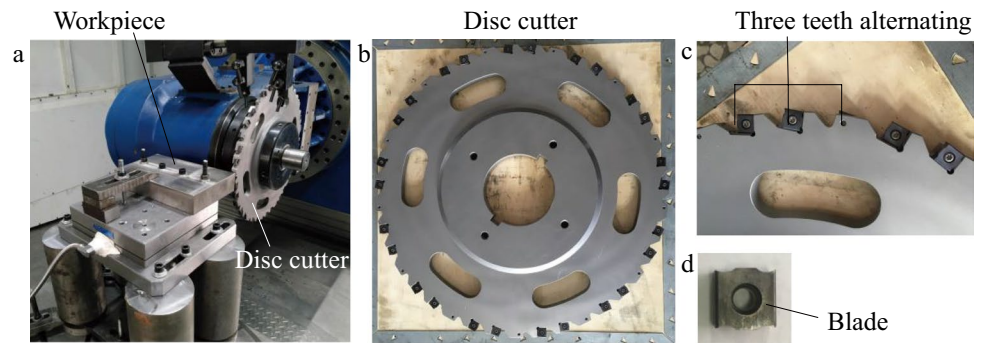
$$T_j = T_i \times \frac{\eta(X_i)}{\eta(X_j)} \tag{4}$$

It can be seen that if the above conjecture is verified, it will provide a very practical tool wear prediction method for related research and actual cutting production. It can quickly predict the tool wear value and tool life under a certain cutting parameter, and is not limited by the machining type, machining method, workpiece material and tool type, so it has good universality and application value.

3 Modeling of wear influence factor $\eta(X)$ through experiments

The experimental platform in this paper is the disc milling grooving machine tool. One of the characteristics of disc milling grooving is that its cutting width is equal to the thickness of the disc tool [28], so the cutting width is constant and will not change during the disc milling process. Therefore, there are only two cutting variables for disc milling, namely, cutting line speed V and feed per tooth a_p .

Fig. 3 Disc milling process, disc cutter, the blade and distribution mode



Because of this, it is simpler to solve the relationship model between the tool wear rate and cutting parameters than the machining methods with multiple cutting variables. The disc cutter and the process of disc milling are shown in Fig. 3.

The diameter of the disc cutter body is 420 mm, and it has 39 cutter teeth in all. Every three cutter teeth are in a group, which are arranged in order of right, middle and left, so there are 13 right teeth, middle teeth and left teeth respectively, as shown in Fig. 3(c) and Fig. 4. Blades are installed on the disc cutter in a replaceable way, for each blade, four cutting edges are symmetrically designed, and each cutting edge has circular arc ovlume crumbs slot. The workpiece material is TC17 titanium alloy, and the size of each workpiece is 270×170×50(mm), as shown in Fig. 4(d). The blade material is WC-Co cemented carbide, the size of blade is 12.7×12.7×6 (mm), the rake angle α_r of disc milling is 8°, as shown in Fig. 4(c) and Fig. 5.

As an efficient roughing method, disc milling has the characteristics of high cutting force and high cutting temperature [28, 29]. Therefore, compared with ordinary milling, the tool wear rate of disc milling is faster, especially in the case of poor cooling. In order to be consistent with the disc milling processing conditions in the actual production, this experiment uses coolant as the cooling method.

In order to obtain an accurate model, this paper will derive $\eta(X)$ through tool wear cutting experiments. The specific method is to carry out regression analysis on the basis of the tool wear experimental data under different cutting parameters to obtain the relationship function between the tool wear rate and the cutting parameters, then remove the factors irrelevant to cutting parameters in the function, and the remaining part is the tool wear influence factor $\eta(X)$. After obtaining $\eta(X)$, carry out the tool wear life experiment, and record the curve of tool wear value over machining time

Fig. 4 Disc cutter and workpiece. (a) The overall picture; (b) the enlarged view of three teeth alternating; (c) the blade size (d) the workpiece size

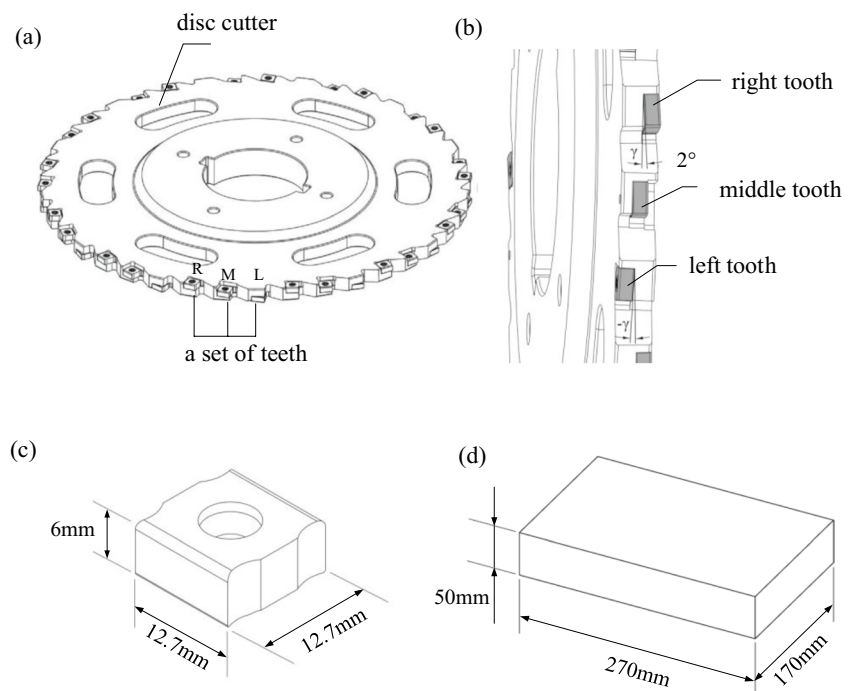
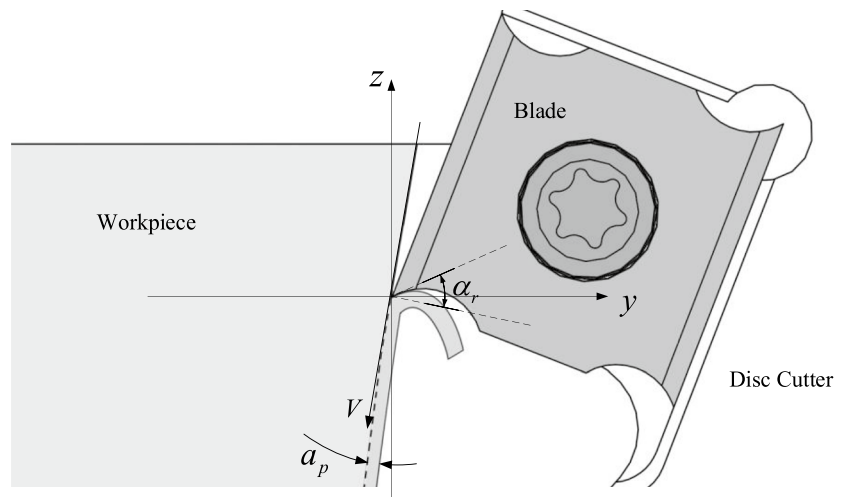


Fig. 5 Geometric parameters of disc milling



under a certain set of cutting parameters, which is called the benchmark tool wear curve $VB_s(t)$. This set of cutting parameters is called the benchmark cutting parameters X_s , and the tool wear influence factor under X_s is called the benchmark wear influence factor $\eta(X_s)$. When the cutting parameters change, it is only necessary to calculate the tool wear influence factor $\eta(X_p)$ under the current cutting parameters X_p , then calculate the scaling ratio $\lambda_{s,p} = \frac{\eta(X_p)}{\eta(X_s)}$. The tool wear prediction curve $VB_p(t)$ under the current cutting parameters X_p can be obtained by stretching or compressing $VB_s(t)$ in the direction of the abscissa according to the value of $\lambda_{s,p}$.

When solving the relationship model between a single target and multiple parameters that change continuously, when the relationship between the parameters is relatively independent and there is no mutual influence or the degree of mutual influence is very weak, the multivariate power function regression shown in Eq. (5) has good regression effect and accuracy.

$$S_{VB}(X) = 10^\omega \times x_1^k \times x_2^m \times \dots \times x_n^q \tag{5}$$

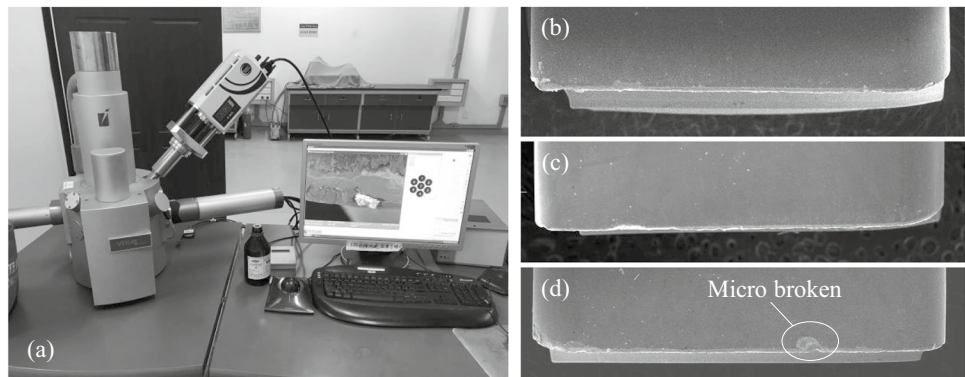
where $S_{VB}(X)$ is the tool wear rate function, ω, k, m, \dots, q are the power of each cutting parameter variable.

Since there are only two cutting variables for disc milling grooving, in this cutting experiment, there are only two variable parameters in the set X , where x_1 is the cutting line speed V , and x_2 is the feed per tooth a_p , as shown in Fig. 5, so the regression analysis of disc milling tool wear can adopt the binary power function shown in Eq. (6).

$$S_{VB}(X) = 10^\omega \times V^k \times a_p^m \tag{6}$$

Since the cutting width of the disc milling cutter is composed of three adjacent blades, as shown in Fig. 3(c) and Fig. 4, there will be a joint in the cutting width of every two adjacent blades, and the cutting edge is prone to damage at the position of the joint, which is called micro-broken, as shown in Fig. 6. Micro-broken can interfere with the measurement of tool flank wear and can affect the cutting ability of the cutting edge, and blades with micro-broken will wear out faster. It is found that the occurrence of micro-broken is related to the position of the blade installed on the disc cutter. Since the disc cutter has 39 positions for installing the blade, we can select the position where the cutting edge is not easily damaged as the installation position of the experimental blade.

Fig. 6 SEM photos of disc milling tool wear



The width of the even flank wear is used as the measurement value of tool wear in the experiment, and the measurement equipment is MIRA3 XMU scanning electron microscope (SEM), as shown in Figs. 6 and 7. The measurement of the flank wear value was carried out by taking the average of three measurements.

In the case of only two cutting variables, in order to perform power function regression analysis as accurately and comprehensively as possible, a two-factor four-level full combination cutting test was implemented. According to the milling experience of titanium alloy TC17 disc milling, the commonly used range of cutting linear speed V is 30–90 m/min, and the commonly used range of feed per tooth a_p is 0.06–0.18 mm/tooth. There are 16 experimental groups in total, and the tool wear value VB is measured after cutting for 10 min in each test.

The test groups and tool wear results of Experiment 1 are shown in Table 1.

Based on Eq. (6), the binary power function regression is performed on the experimental data in Table 1, and the regression result is $\omega = 2.4264$, $k = 0.2972$, $m = 1.4806$, as shown in Eq. (7).

$$S_{VB}(X) = 10^{2.4264} \times V^{0.2972} \times a_p^{1.4806} \quad (7)$$

Since the machining time of each group in Table 1 is the same, the amount of tool wear under a certain group of cutting parameters actually represents the tool wear rate under this group of cutting parameters. After removing the constant factor in Eq. (7), the remaining factor that only includes cutting parameters is the wear influence factor $\eta(X)$, as shown in Eq. (8).

$$\eta(X) = V^{0.2972} a_p^{1.4806} \quad (8)$$

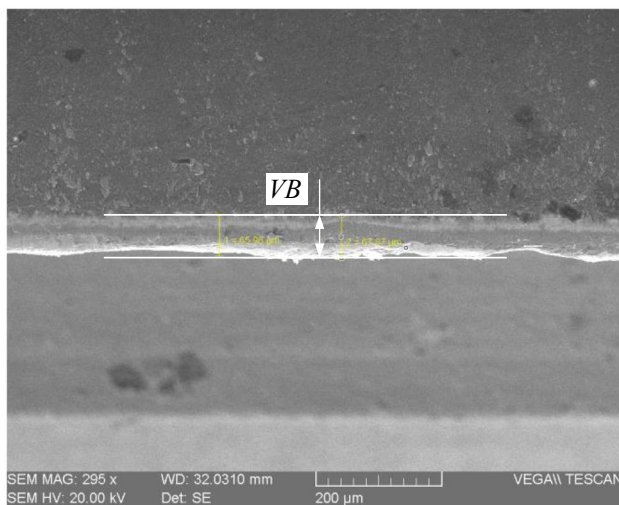


Fig. 7 Measurement of disc milling tool wear

Table 1 Experiment on relationship between tool wear and cutting parameters (Experiment 1)

Number of test	Cutting linear speed V (m/min)	Feed per tooth a_p (mm/tooth)	Tool wear value VB (μ m)
1	30	0.06	11.39
2	30	0.10	24.23
3	30	0.14	39.92
4	30	0.18	57.88
5	50	0.06	13.28
6	50	0.10	28.20
7	50	0.14	46.47
8	50	0.18	67.38
9	70	0.06	14.66
10	70	0.10	31.19
11	70	0.14	51.33
12	70	0.18	74.48
13	90	0.06	15.79
14	90	0.10	33.60
15	90	0.14	55.34
16	90	0.18	80.25

The image of $\eta(X)$ can be drawn with Matlab, as shown in Fig. 8.

$\eta(X)$ is positively correlated with the cutting linear speed V and the feed per tooth a_p , but obviously, the influence of the feed per tooth a_p is much greater than the cutting linear speed V . This result is easier to understand in disc milling for the following reasons:

According to the cutting and wear mechanism [29] [30], tool wear is positively correlated with cutting temperature and cutting force. If the feed per tooth a_p is increased while the cutting line speed V remains constant, both the cutting force and the cutting temperature will increase. If the feed per tooth a_p is unchanged, only the cutting linear speed V is

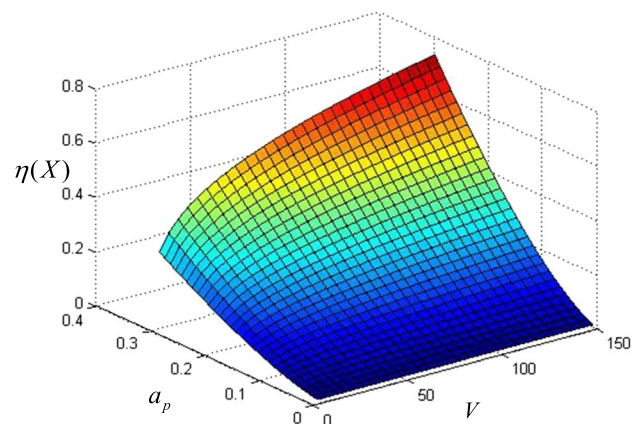


Fig. 8 The image of $\eta(X)$

increased, and the cutting force will not be affected much. As for the cutting temperature, since the disc cutter has 39 teeth, each tooth only participates in short-term intermittent cutting. Although the increase of the cutting linear speed will speed up the cutting heat generation, it also shortens the time for each tooth to participate in a single cutting, so that the cutting edge can quickly pass through the cutting area. This reduces the time for cutting heat generation, so the increase in cutting temperature of each tooth is limited.

In addition, as shown in Fig. 9, according to the geometric characteristics of disc milling, the ratio of the cutting time t_M of each tooth to the cooling time t_C can be calculated by Eq. (9).

$$\begin{cases} \frac{t_M}{t_C} = \frac{2\theta_w}{2\pi - 2\theta_w} \\ \theta_w = \arcsin \frac{H}{2R} \end{cases} \quad (9)$$

where $H=50\text{mm}$, $R=210\text{mm}$, so $\frac{t_M}{t_C} \approx \frac{1}{25}$. Therefore, even with an increased cutting line speed, each tooth has sufficient cooling time. Combining the above reasons, it explains why the feed per tooth a_p has a much greater influence on tool wear than the cutting line speed V .

It should be noted that when modeling $\eta(X)$ in this paper, the range of cutting linear speed V is 30-90m/min, and the range of feed per tooth a_p is 0.06-0.18mm/z. Therefore, when using $\eta(X)$ to predict the tool wear rate under different cutting parameters, the cutting parameters should also be within the above range, which is called the effective parameter interval X_{EPI} , as shown in Eq. (10).

$$X_{EPI} = \{(V, a_p) | 30 \leq V \leq 90(m/\text{min}), 0.06 \leq a_p \leq 0.18(\text{mm}/\text{tooth})\} \quad (10)$$

4 Disc milling tool wear curve prediction model and its experimental verification

4.1 Disc milling tool wear curve prediction model

In order to obtain the benchmark tool wear curve $VB_s(t)$ of disc milling, it is necessary to select a set of parameters as the benchmark cutting parameters X_s , and then conduct tool wear experiments under X_s . During the experiment, the flank wear value needs to be recorded at intervals, and the recorded wear data can be used to draw the tool wear curve, which is the benchmark tool wear curve $VB_s(t)$.

In this experiment, the cutting tools, workpieces, and cooling conditions are all consistent with Experiment 1, and the selected X_s is: $V=55\text{m}/\text{min}$, $a_p=0.08\text{mm}/\text{tooth}$. The tool flank wear is measured every 20 minutes during machining until the wear value exceeds the blunt standard, that is, the flank wear reaches 0.3mm [14] [29]. The tool wear measurement data corresponding to X_s is referred to as $VB_s(M)$, and the experimental results are shown in the Table 2.

Take the machining time t as the abscissa and the tool flank wear VB as the ordinate, draw the data of $VB_s(M)$ in Table 2 into a scattered line chart, as shown in Fig. 10(a).

The polynomial function is used to fit the $VB_s(M)$, and it is found that the curve obtained by the quartic polynomial fitting is relatively consistent with $VB_s(M)$, as shown in Fig. 10(b), and the fitting function is exactly the $VB_s(t)$, proposed above, as shown in Eq. (11).

$$VB_s(t) = -40.5845 + 4.7527t - 0.0556t^2 + 2.8949 \times 10^{-4} \times t^3 - 4.8560 \times 10^{-7} \times t^4 \quad (11)$$

Fig. 9 Disc milling geometry

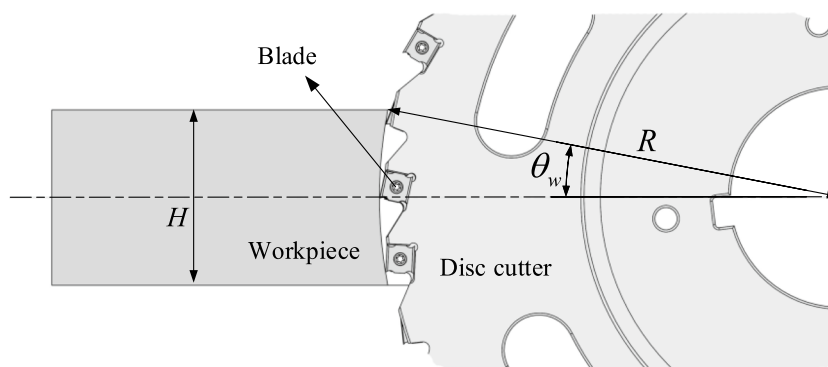
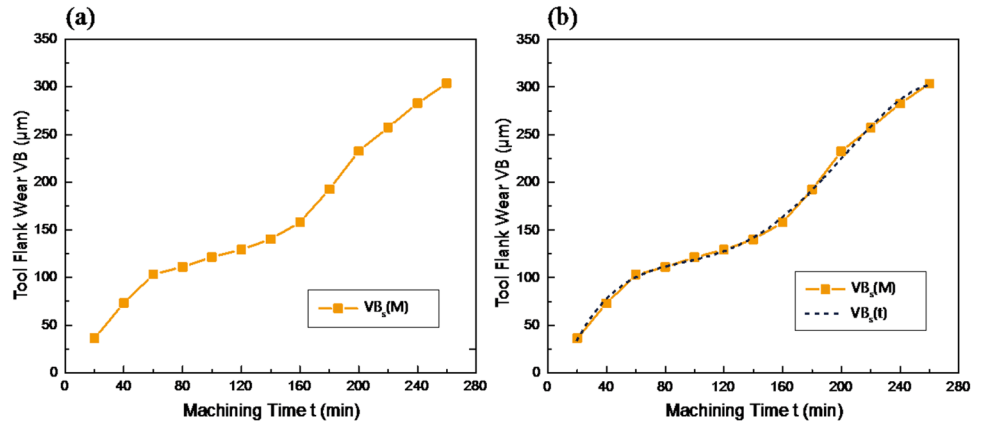


Table 2 Tool wear measurement data under X_s (Experiment 2)

Machining time (min)	20	40	60	80	100	120	140
Flank wear value (μm)	36.23	73.18	103.26	111.05	121.47	129.34	140.29
Machining time (min)	160	180	200	220	240	260	
Flank wear value (μm)	158.06	192.31	226.56	257.35	282.72	303.61	

Fig. 10 Data line chart of $VB_s(M)$. (a) Line chart; (b) line chart and its fitting curve



$\eta(X_s)$ corresponding to $VB_s(t)$ is given as:

$$\eta(X_s) = 55^{0.2972} \times 0.08^{1.4806} = 0.0782 \tag{12}$$

Choosing a set of parameters as the current cutting parameter X_p within the effective parameter interval X_{EPI} , and its corresponding wear influence factor is $\eta(X_p)$, then the scaling ratio $\lambda_{s,p}$ can be given as:

$$\lambda_{s,p} = \frac{\eta(X_p)}{\eta(X_s)} = \frac{\eta(X_p)}{0.0782} \tag{13}$$

After the expression of $\lambda_{s,p}$ is obtained, the tool wear curve $VB_p(t)$ under X_p can be predicted by the tool wear prediction model proposed in this paper, as shown in Eq. (14), which is the final form of the TC17 titanium alloy disc milling tool wear curve prediction model.

$$VB_p(t) = -40.5845 + 4.7527 \left(\frac{\eta(X_p)}{0.0782} t \right) - 0.0556 \left(\frac{\eta(X_p)}{0.0782} t \right)^2 + 2.8949 \times 10^{-4} \times \left(\frac{\eta(X_p)}{0.0782} t \right)^3 - 4.8560 \times 10^{-7} \times \left(\frac{\eta(X_p)}{0.0782} t \right)^4 \tag{14}$$

4.2 Experimental verification of disc milling tool wear curve prediction model

Two sets of cutting parameters X_{p1} and X_{p2} are selected for the verification experiment, where X_{p1} is $V=80m/min, a_p=0.12mm/tooth$, and X_{p2} is $V=40m/min, a_p=0.06mm/tooth$. $\eta(X_{p1})$ and $\eta(X_{p2})$ are given as:

$$\eta(X_{p1}) = 80^{0.2972} \times 0.12^{1.4806} = 0.1593 \tag{15}$$

$$\eta(X_{p2}) = 40^{0.2972} \times 0.06^{1.4806} = 0.04646 \tag{16}$$

$\lambda_{s,p1}$ and $\lambda_{s,p2}$ are given as:

$$\lambda_{s,p1} = \frac{\eta(X_{p1})}{\eta(X_s)} = \frac{0.1593}{0.0782} = 2.0371 \tag{17}$$

$$\lambda_{s,p2} = \frac{\eta(X_{p2})}{\eta(X_s)} = \frac{0.04646}{0.0782} = 0.5941 \tag{18}$$

According to Eq. (14), the function expressions of the tool wear prediction curve under X_{p1} and X_{p2} can be obtained, as shown in Eq. (19) and Eq. (20).

$$VB_{p1}(t) = -40.5845 + 4.7527 \times (2.0371t) - 0.0556 \times (2.0371t)^2 + 2.8949 \times 10^{-4} \times (2.0371t)^3 - 4.8560 \times 10^{-7} \times (2.0371t)^4 \tag{19}$$

$$VB_{p2}(t) = -40.5845 + 4.7527 \times (0.5941t) - 0.0556 \times (0.5941t)^2 + 2.8949 \times 10^{-4} \times (0.5941t)^3 - 4.8560 \times 10^{-7} \times (0.5941t)^4 \tag{20}$$

Except for the different cutting parameters, the experimental conditions of the verification experiments under X_{p1} and X_{p2} are exactly the same as those of Experiment 2. Since the value of $\eta(X_{p1})$ is about twice that of $\eta(X_s)$, it is guessed that the tool wear rate under X_{p1} will be much faster than that under X_s , so the measurement interval of the flank wear value of X_{p1} is changed to every 10 minutes. Similarly, the value of $\eta(X_{p2})$ is much smaller than that of $\eta(X_s)$, it is guessed that the tool wear rate under X_{p2} will be slower than that under X_s , so the measurement interval of the flank wear value of X_{p2} is changed to every 30 minutes.

The tool wear measurement data corresponding to X_{p1} is referred to as $VB_{p1}(M)$, and the experimental results under X_{p1} are shown in Table 3.

The tool wear measurement data corresponding to X_{p2} is referred to as $VB_{p2}(M)$, and the experimental results under X_{p2} are shown in Table 4.

The benchmark tool wear curve $VB_s(t)$, the tool wear prediction curve $VB_{p1}(t)$ under X_{p1} , and $VB_{p2}(t)$ under X_{p2} are all drawn in Fig. 11(a). In this figure, the relationship between $VB_s(t)$, $VB_{p1}(t)$ and $VB_{p2}(t)$ can be observed intuitively. According to the principle of function stretching and compressing, since $\lambda_{s, p1} > 1$, $VB_{p1}(t)$ is the result of

Table 3 Tool wear measurement data under X_{p1} (Experiment 3)

Machining time (min)	10	20	30	40	50	60	70
Flank wear value (μm)	38.54	72.69	108.27	119.14	127.52	137.88	150.36
Machining time (min)	80	90	100	110	120	130	130
Flank wear value (μm)	173.73	193.58	239.81	261.17	290.79	315.58	

Table 4 Tool wear measurement data under X_{p2} (Experiment 4)

Machining time (min)	30	60	90	120	150	180	210
Flank wear value (μm)	34.35	80.91	99.76	106.30	111.24	119.55	134.72
Machining time (min)	240	270	300	330	360	390	420
Flank wear value (μm)	152.59	173.46	185.28	226.55	254.29	288.33	309.86

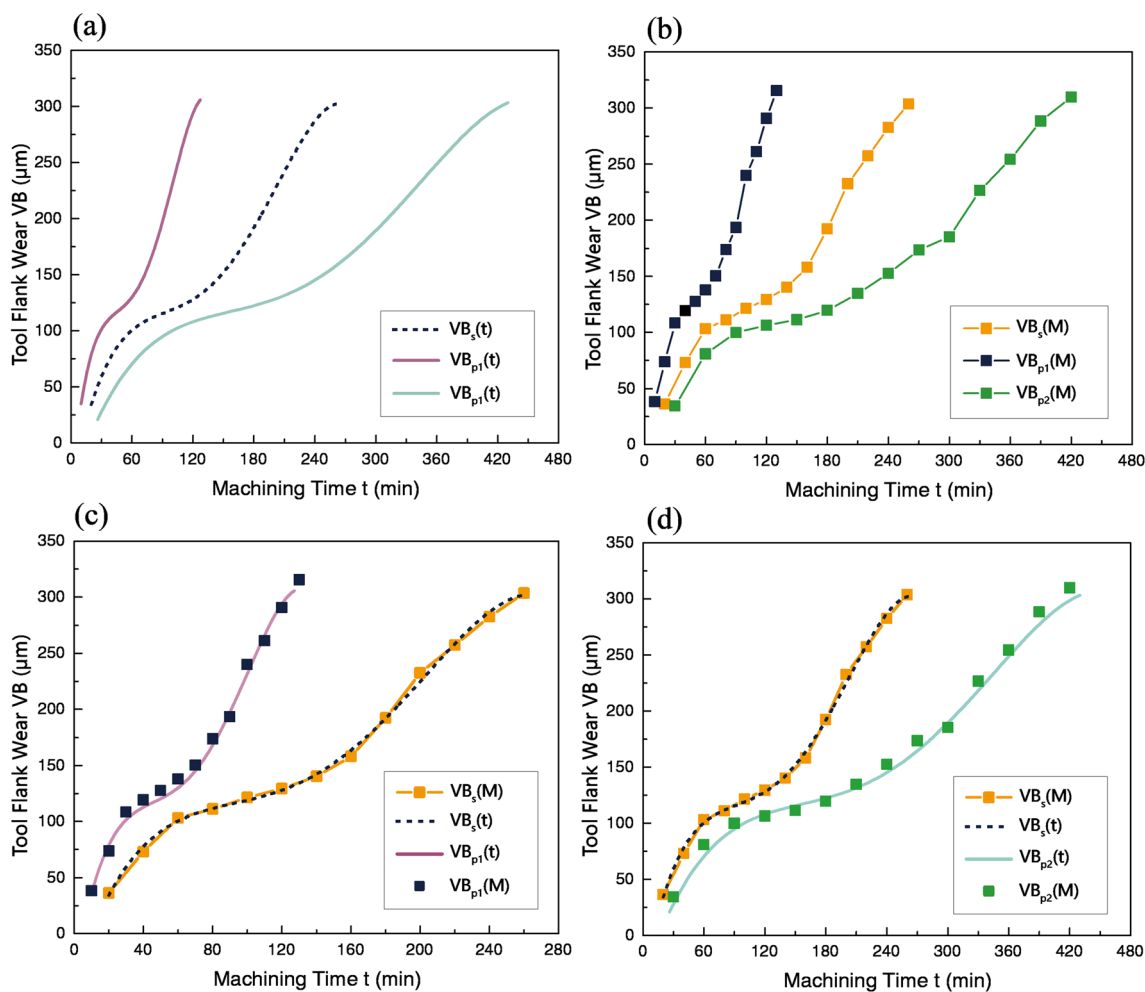


Fig. 11 Comparison of tool wear prediction curves with experimental measurement data

compressing the abscissa by $\lambda_{s,p1}$ times on the basis of $VB_s(t)$. And $\lambda_{s,p2} < 1$, so $VB_{p2}(t)$ is the result of stretching the abscissa by $1/\lambda_{s,p2}$ times based on $VB_s(t)$.

$VB_s(M)$, $VB_{p1}(M)$, and $VB_{p2}(M)$ are actual measurement data of tool wear over time, corresponding to cutting parameters X_s , X_{p1} , and X_{p2} respectively. Draw the line graphs of the three in Fig. 11(b), it can be seen that the positions, shapes, and trends of the three are almost consistent with the three curves in Fig. 11(a).

Figure 11(c) and (d) compared the tool wear prediction curve with the actual measurement data more intuitively, and found that both $VB_{p1}(t)$ and $VB_{p2}(t)$ have a very high consistency with the actual tool wear measurement data, which shows that the prediction results are accurate and reliable. Therefore, the abscissa stretching and compressing tool wear prediction model based on tool wear influencing factors proposed in this paper is effective.

In addition, the tool life prediction model proposed in this paper is directly derived on the basis of the tool wear influence factor and the tool wear prediction curve model. Therefore, when the latter two are verified by experiments, the tool life prediction model is naturally verified.

4.3 Method flowchart of establishing the tool wear prediction model

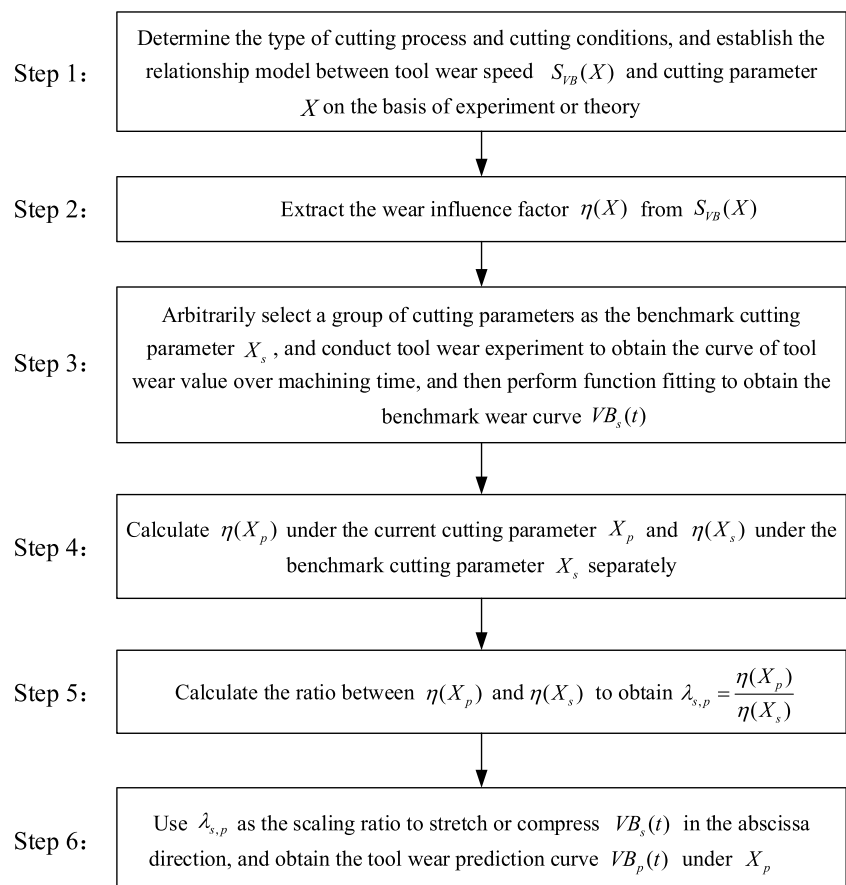
In order to more clearly describe the modeling process and method, Fig. 12 shows the modeling steps of the tool wear prediction model with abscissa scaling based on wear influence factor through flowchart.

4.4 Cross-validation of the prediction model

When establishing the tool wear prediction model in this paper, the selection of the benchmark tool wear curve is arbitrary. Therefore, in order to verify the effectiveness of the prediction model, the selection of the benchmark tool wear curve needs to be replaced for cross validation, so as to prove that the arbitrary selection of the benchmark tool wear curve will not affect the effectiveness of the tool wear prediction model.

In this cross-validation, the tool wear curve under cutting parameter X_{p2} ($V=40\text{m/min}$, $a_p=0.06\text{mm/tooth}$) is selected as the second benchmark tool wear curve, and the polynomial function is also used to fit it, then the expression of the second benchmark tool wear curve $VB_{p2,s}(t)$ can be obtained as follows:

Fig. 12 Method flowchart of establishing the tool wear prediction model



$$\begin{aligned}
 VB_{p2,s}(t) = & -24.2614 + 2.5584 \\
 & t - 0.0182t^2 \\
 & + 5.7520 \times 10^{-5} \times t^3 \\
 & - 5.7830 \times 10^{-8} \times t^4
 \end{aligned}
 \tag{21}$$

$VB_{p2,s}(t)$ and the corresponding tool wear measurement data $VB_{p2,s}(M)$ are shown in Fig. 13(a).

According to the prediction model proposed in this paper, when the cutting parameter is $X_s(V=55\text{m/min}, a_p=0.08\text{mm/tooth})$, the corresponding scaling ratio $\lambda_{p2,s} = \frac{\eta(X_s)}{\eta(X_{p2})} = 1.6832$, then the tool wear prediction curve $VB_{s,p2}(t)$ can be obtained by compressing $VB_{p2,s}(t)$ $\lambda_{p2,s}$ times in the abscissa direction, as shown in Eq. (22).

$$\begin{aligned}
 VB_{s,p2}(t) = & -24.2614 + 2.5584 \times (1.6832t) - 0.0182 \times (1.6832t)^2 + \\
 & 5.7520 \times 10^{-5} \times (1.6832t)^3 - 5.7830 \times 10^{-8} \times (1.6832t)^4
 \end{aligned}
 \tag{22}$$

And when the cutting parameter is $X_{p1}(V=80\text{m/min}, a_p=0.12\text{mm/tooth})$, the corresponding scaling ratio $\lambda_{p2,p1} = \frac{\eta(X_{p1})}{\eta(X_{p2})} = 3.4288$, then the tool wear prediction curve $VB_{p1,p2}(t)$ can be obtained by compressing $VB_{p2,s}(t)$ $\lambda_{p2,p1}$ times in the abscissa direction, as shown in Eq. (23).

$$\begin{aligned}
 VB_{p1,p2}(t) = & -24.2614 \\
 & + 2.5584 \times (3.4288t) - 0.0182 \times (3.4288t)^2 \\
 & + 5.7520 \times 10^{-5} \times (3.4288t)^3 - 5.7830 \\
 & \times 10^{-8} \times (3.4288t)^4
 \end{aligned}
 \tag{23}$$

$VB_{p2,s}(t)$, $VB_{p1,p2}(t)$ and the corresponding tool wear measurement data $VB_{p2,s}(M)$, $VB_{p1,p2}(M)$ are shown in Fig. 13(b).

It can be found that in the cross-validation after the replacement of the benchmark tool wear curve, the predicted tool wear results still match the actual tool wear measurement data very

well, which proves that the arbitrary selection of the benchmark tool wear curve will not affect the effectiveness of the tool wear prediction model proposed in this paper.

4.5 Optimization of cutting parameters based on prediction model

According to actual production needs, the optimization goal of disc milling is not only to reduce tool wear, but also to improve cutting efficiency. Cutting efficiency is generally characterized by material removal rate, and the expression for material removal rate Q during disc milling can be given as:

$$Q = \frac{V_f \times H \times a_e}{1000}
 \tag{24}$$

where V_f is the feed speed, H is the thickness of the work-piece, and a_e is the thickness of the disc cutter. According to the cutting characteristics of disc milling, there is a relationship between feed speed V_f , feed per tooth a_p , and cutting line speed V as shown in Eq. (25):

$$V_f = 13 \times \frac{V \times a_p}{2\pi R}
 \tag{25}$$

So the expression for material removal rate Q can be given as:

$$Q = \frac{13 \times H \times a_e}{1000 \times 2\pi R} \times V \times a_p
 \tag{26}$$

where the left part $\frac{13 \times H \times a_e}{1000 \times 2\pi R}$ is a constant.

A function $\eta_{op}(X)$ is introduced to characterize the comprehensive optimization of disc milling cutting, as shown in Eq. (27).

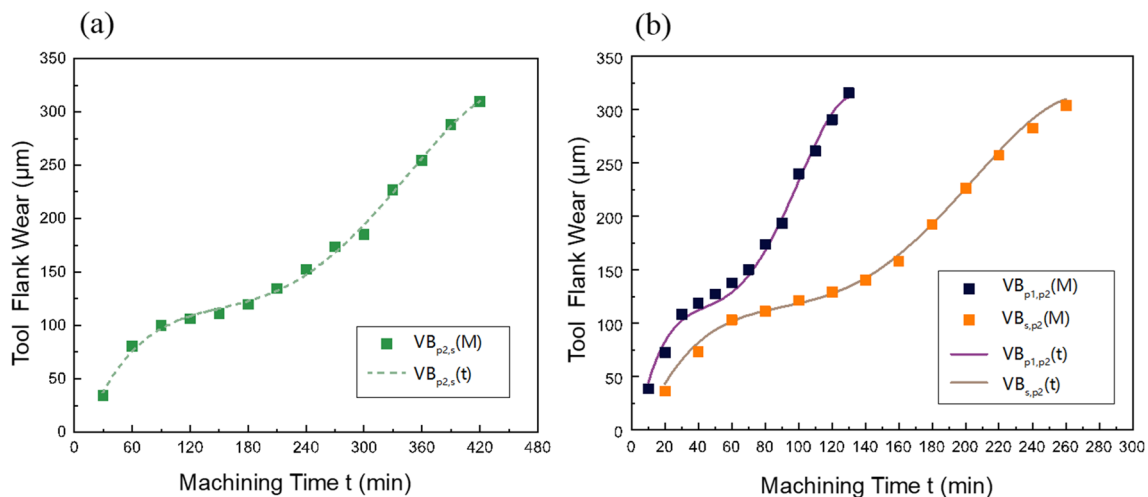


Fig. 13 Comparison of tool wear prediction curves with experimental measurement data in cross-validation

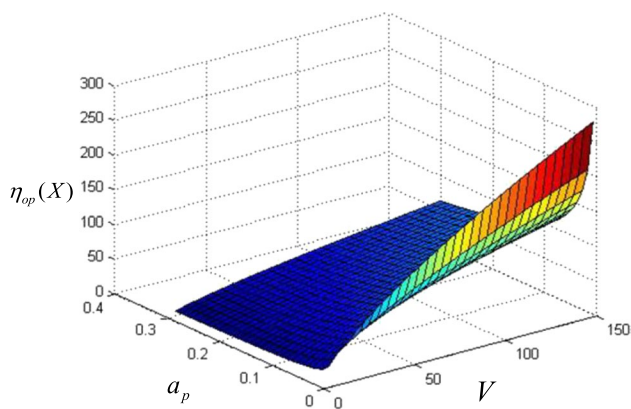


Fig. 14 The image of $\eta_{op}(X)$

$$\eta_{op}(X) = \frac{V \times a_p}{\eta(X)} \tag{27}$$

According to Eq. (26), the numerator $V \times a_p$ of Eq. (27) represents the material removal rate, that is, the cutting efficiency, and the denominator $\eta(X)$ is the characterization factor of tool wear rate. Obviously, when $\eta_{op}(X)$ takes the maximum value, the comprehensive cutting effect is optimal, because in this case, the cutting efficiency is high and the tool wear speed is slow.

$\eta_{op}(X)$ can be given as:

$$\eta_{op}(X) = \frac{V \times a_p}{V^{0.2972} a_p^{1.4806}} = V^{0.7028} a_p^{-0.4806} \tag{28}$$

The image of $\eta_{op}(X)$ is shown in Fig. 14.

In this paper, the tool wear prediction model of disc milling is established based on the tool wear influence factor $\eta(X)$. Therefore, when the tool wear prediction model is verified, it is equivalent to the tool wear influence factor $\eta(X)$ being verified. The comprehensive optimization function $\eta_{op}(X)$ of disc milling is directly derived from $\eta(X)$, so it is also verified.

According to Eq. (28) and Fig. 14, it is obvious that the cutting line speed V is positively correlated with $\eta_{op}(X)$, while feed per tooth a_p is negatively correlated with $\eta_{op}(X)$. Therefore, when comprehensively optimizing the cutting efficiency and tool wear of disc milling, the cutting line speed should be increased and the feed per tooth should be appropriately reduced.

5 Discussion

5.1 Effective interval of independent variable of the prediction model

It should be noted that since $VB_s(t)$ is obtained by polynomial fitting, one of the characteristics of polynomial fitting is

that within the sample interval of the independent variable, the fitting value and the actual value are very consistent. However, outside the sample interval of the independent variable, there may be a very large deviation between the fitting value and the actual value. Since $VB_{p1}(t)$ and $VB_{p2}(t)$ are obtained by compressing or stretching $VB_s(t)$ in the direction of the abscissa, when using $VB_{p1}(t)$ or $VB_{p2}(t)$ to predict the tool wear curve, the valid interval of the corresponding independent variable will also be limited by the sample interval of the independent variable of $VB_s(t)$. Define the sample interval of $VB_s(t)$ as t_s , the effective interval of the independent variable of $VB_{p1}(t)$ as t_{p1} , and the effective interval of the independent variable of $VB_{p2}(t)$ as t_{p2} . From the data sample of Experiment 1, it can be seen that $t_s = \{t | 20 \leq t \leq 260(\text{min})\}$. Then according to the characteristics of the function compressing or stretching, t_{p1} and t_{p2} can be given by:

$$t_{p1} = \left\{ t \mid \frac{20}{\lambda_{s,p1}} \leq t \leq \frac{260}{\lambda_{s,p1}}(\text{min}) \right\} = \{t | 9.82 \leq t \leq 127.63(\text{min})\} \tag{29}$$

$$t_{p2} = \left\{ t \mid \frac{20}{\lambda_{s,p2}} \leq t \leq \frac{260}{\lambda_{s,p2}}(\text{min}) \right\} = \{t | 33.66 \leq t \leq 437.64(\text{min})\} \tag{30}$$

5.2 Error analysis of the prediction model

When the tool wear curve under cutting parameter $X_s(V=55\text{m/min}, a_p=0.08\text{mm/tooth})$ is selected as the benchmark wear curve, by comparing the actual tool wear measurement data with the prediction results and calculating the relative error, it is found that when the cutting parameter is $X_{p1}(V=80\text{m/min}, a_p=0.12\text{mm/tooth})$, the prediction relative

Table 5 Repetitive error experiments

Machining time (min)	Flank wear value (μm)		
	Repeat test 1	Repeat test 2	Repeat test 3
20	36.23	35.47	36.31
40	73.18	71.74	73.66
60	103.26	101.45	102.80
80	111.05	110.82	112.97
100	121.47	119.59	123.06
120	129.34	127.90	131.23
140	140.29	138.67	141.45
160	158.06	155.95	157.30
180	192.31	188.24	190.28
200	226.56	221.70	224.12
220	257.35	253.41	260.63
240	282.72	277.38	285.10
260	303.61	299.56	306.72

error is between 0.93% and 8.63%. When the cutting parameter is X_{p2} ($V=40\text{m/min}$, $a_p=0.06\text{mm/tooth}$), the prediction relative error of the first two data in the initial wear stage is slightly larger, which may be caused by the instability of tool wear in the initial wear stage, but from the third data, the prediction relative error is all within 5%.

In the cross validation of the prediction model, the prediction results are also accurate. When predicting the tool wear curve under cutting parameters X_s and X_{p1} , only the first two data in the initial wear stage have a slightly larger prediction relative error. From the third data, the relative error is all within 5%. Therefore, the selection of the benchmark tool wear curve will not affect the accuracy and effectiveness of the tool wear prediction model proposed in this paper.

In addition, in order to verify the repetitive error of tool wear in disc milling, repeated cutting experiments were carried out when the cutting parameter was X_s . The experimental result shows that when the cutting conditions, cutting parameters, and the installation position of the blade are all the same, there is a high degree of consistency between tool wear curves in the repeated cutting experiments, and the repeated error is within 3%, as shown in Table 5. Therefore, it can be believed that the impact of repeated error on the accuracy of the prediction model proposed in this paper can be ignored.

6 Conclusion

This study proposed a tool wear prediction model with abscissa stretching or compressing based on wear influence factor. In this model, the tool wear prediction curve under current cutting parameters can be obtained by stretching or compressing the benchmark tool wear curve in the direction of the abscissa according to the scaling ratio, which is the ratio between the wear influence factor under current cutting parameters and the benchmark wear influence factor. The tool wear curve prediction method proposed in this paper does not depend on a specific cutting equipment and specific cutting condition, it is a prediction method with universally applicable potential, which can be applied to various cutting scene: different machine tools, different tools, different workpieces, and different cutting conditions can all use the method proposed in this paper to predict the tool wear curve.

In the experimental verification of the prediction model, the accuracy and reliability of the tool wear prediction model proposed in this paper are verified. Except for a small number of prediction results that have certain deviation from the experimental data in the initial wear stage, in other wear stages, the relative error between the prediction results and the actual tool wear measurement data is within

5%. In addition, in the cross-validation after the replacement of the benchmark tool wear curve, the prediction model still showed good prediction accuracy and effectiveness, which indicates that the selection of the benchmark tool wear curve can be arbitrary and will not affect the effectiveness of the tool wear prediction model proposed in this paper.

According to the disc milling comprehensive optimization function derived from the prediction model, when comprehensively optimizing the cutting efficiency and tool wear of disc milling, the cutting line speed should be increased and the feed per tooth should be appropriately reduced.

The benchmark tool wear curve in this study was fitted using a polynomial function, so it is necessary to pay attention to the effective interval of the independent variable when using this prediction model. Due to the characteristics of polynomial function fitting, outside the effective interval of the independent variable, the predicted data of the model will quickly deviate from the actual results. Therefore, before using this prediction model, it is necessary to determine the effective independent variable interval of the prediction model according to the method provided in this paper.

Author contribution All authors contributed to the study conception and design. The experiments are designed and carried out mainly by Yang Cheng. The experimental guidance, equipment and funding is done by Shi Yaoyao. The first draft of the manuscript was written by Yang Cheng, Xin Hongmin and Zhao Tao provided a lot of help for the writing and improvement of the manuscript. Zhang Nan and Xian Chao provided assistance for the experiments. All authors commented on previous versions of the manuscript. All authors read and approved the final manuscript.

Funding information This work was supported by the Project Funded by the National Numerical Control Major Projects Foundation of China (Grant No. 2013ZX04001081), China Postdoctoral Science Foundation (Grant No: 2018M631195). Hubei Province Technology Innovation Project (Grant No: 2017AAA133).

Declarations

Ethics approval and consent to participate The research does not involve human participants and/or animals.

Consent for publication The publication has been approved by all authors.

Competing interests The authors declare no competing interests.

References

1. Taylor FW (1907) On the art of cutting metals. The Am Soc Mech Eng. <http://ir.library.oregonstate.edu/downloads/d791sn02d>. Accessed 11 May 2023
2. Archard JF (1953) Contact and Rubbing of Flat Surfaces. J Appl Phys 24(8):981–988. <https://doi.org/10.1063/1.1721448>

3. Colding BN (1959) A Three-Dimensional Tool Life Equation - Machining Economics. *J Eng Ind* 81(3):239–250. <https://doi.org/10.1115/1.4008313>
4. Usui E, Shirakashi T, Kitagawa T (1984) Analytical prediction of cutting tool wear. *Wear* 100(1–3):129–151. [https://doi.org/10.1016/0043-1648\(84\)90010-3](https://doi.org/10.1016/0043-1648(84)90010-3)
5. Chetan, Narasimhulu A, Ghosh S, Rao PV (2015) Study of Tool Wear Mechanisms and Mathematical Modeling of Flank Wear During Machining of Ti Alloy (Ti6Al4V). *J Inst Eng (India): Series C* 96:279–285. <https://doi.org/10.1007/s40032-014-0162-9>
6. He GH, Liu XL, Wen X, Wu CH, Li LX (2017) An investigation of the destabilizing behaviors of cemented carbide tools during the interrupted cutting process and its formation mechanisms. *Int J Adv Manuf Technol* 89:1959–1968. <https://doi.org/10.1007/s00170-016-9245-5>
7. Mao Z, Luo M, Zhang DH (2022) Tool wear prediction at different cutting edge locations for ball-end cutter in milling of Ni-based superalloy freeform surface part. *Int J Adv Manuf Technol* 120:2961–2977. <https://doi.org/10.1007/s00170-022-08790-4>
8. Aline GS, Marcio BS, Mark JJ (2018) Tungsten carbide micro-tool wear when micro milling UNS S32205 duplex stainless steel. *Wear* 414–415:109–117. <https://doi.org/10.1016/j.wear.2018.08.007>
9. Luo X, Cheng K, Holt R, Liu X (2005) Modeling flank wear of carbide tool insert in metal cutting. *Wear* 259:1235–1240. <https://doi.org/10.1016/j.wear.2005.02.044>
10. Zhang Y, Zhu KP, Duan XY, Li S (2021) Tool wear estimation and life prognostics in milling: Model extension and generalization. *Mech Syst Signal Process* 155:107617. <https://doi.org/10.1016/j.ymsp.2021.107617>
11. Abhishek S, Ghosh S, Aravindan S (2022) Pseudo analytical modelling of flank wear for coated/micro blasted cemented carbide cutting tools. *J Manuf Process* 80:54–68. <https://doi.org/10.1016/j.jmapro.2022.05.053>
12. Chinchankar S, Choudhury SK (2015) Predictive modeling for flank wear progression of coated carbide tool in turning hardened steel under practical machining conditions. *Int J Adv Manuf Technol* 76:1185–1201. <https://doi.org/10.1007/s00170-014-6285-6>
13. Halila F, Czarnota C, Nouari M (2014) A new abrasive wear law for the sticking and sliding contacts when machining metallic alloys. *Wear* 315:125–135. <https://doi.org/10.1016/j.wear.2014.03.013>
14. Laakso S, Johansson D (2019) There is logic in logit – including wear rate in Colding's tool wear model. *Procedia Manuf* 38:1066–1073. <https://doi.org/10.1016/j.promfg.2020.01.194>
15. Zhang X, Gao Y, Guo ZC, Zhang W, Yin J, Zhao WH (2023) Physical model-based tool wear and breakage monitoring in milling process. *Mech Syst Signal Process* 184:109641. <https://doi.org/10.1016/j.ymsp.2022.109641>
16. Kamratowski M, Alexopoulos C, Brimmers J, Bergs T (2023) Model for tool wear prediction in face hobbing plunging of bevel gears. *Wear* 524–525:204787. <https://doi.org/10.1016/j.wear.2023.204787>
17. Zhang C, Zhou L, Liu X (2013) Investigations on model-based simulation of tool wear with carbide tools in milling operation. *Int J Adv Manuf Technol* 64:1373–1385. <https://doi.org/10.1007/s00170-012-4108-1>
18. Li DH, Li YG, Liu CQ (2022) Gaussian process regression model incorporated with tool wear mechanism. *Chinese J Aeronaut* 35(10):393–400. <https://doi.org/10.1016/j.cja.2021.08.009>
19. Wang GF, Qian L, Guo ZW (2013) Continuous tool wear prediction based on Gaussian mixture regression model. *Int J Adv Manuf Technol* 66:1921–1929. <https://doi.org/10.1007/s00170-012-4470-z>
20. Palanisamy P, Rajendran I, Shanmugasundaram S (2008) Prediction of tool wear using regression and ANN models in end-milling operation. *Int J Adv Manuf Technol* 37:29–41. <https://doi.org/10.1007/s00170-007-0948-5>
21. Mandal N, Mondal B, Doloi B (2015) Application of Back Propagation Neural Network Model for Predicting Flank Wear of Yttria Based Zirconia Toughened Alumina (ZTA) Ceramic Inserts. *Trans Indian Inst Met* 68:783–789. <https://doi.org/10.1007/s12666-015-0511-2>
22. Rao KV, Kumar YP, Singh VK, Raju LS, Ranganayakulu J (2021) Vibration-based tool condition monitoring in milling of Ti-6Al-4V using an optimization model of GM(1,N) and SVM. *Int J Adv Manuf Technol* 115:1931–1941. <https://doi.org/10.1007/s00170-021-07280-3>
23. Zhang HY, Zhang C, Zhang JL, Zhou LS (2014) Tool wear model based on least squares support vector machines and Kalman filter. *Prod Eng* 8:101–109. <https://doi.org/10.1007/s11740-014-0527-1>
24. An QL, Tao ZR, Xu XW, Mansori ME, Chen M (2020) A data-driven model for milling tool remaining useful life prediction with convolutional and stacked LSTM network. *Measurement* 154:107461. <https://doi.org/10.1016/j.measurement.2019.107461>
25. Li ZX, Liu XH, Atilla I, Munish KG, Grzegorz MK, Paolo G (2022) A novel ensemble deep learning model for cutting tool wear monitoring using audio sensors. *J Manuf Process* 79:233–249. <https://doi.org/10.1016/j.jmapro.2022.04.066>
26. Binder M, Klocke F, Doebbeler B (2017) An advanced numerical approach on tool wear simulation for tool and process design in metal cutting. *Simul Model Pract Theory* 70:65–82. <https://doi.org/10.1016/j.simpat.2016.09.001>
27. Xin HM, Xing TT, Dai H, Zhang J, Yao CF, Cui MC, Zhang QG (2022) Study on Residual Stress in Disc-Milling Grooving of Blisks. *Materials* 15(20):7261. <https://doi.org/10.3390/ma15207261>
28. Yang C, Shi YY, Xin HM, Zhang N (2021) Milling force model prediction considering tool runout with three-teeth alternating disc cutter. *Int J Adv Manuf Technol* 114:3285–3299. <https://doi.org/10.1007/s00170-021-06949-z>
29. Xin HM, Shi YY, Ning LQ (2016) Tool wear in disk milling grooving of titanium alloy. *Adv Mech Eng* 8(10). <https://doi.org/10.1177/1687814016671620>
30. Altintas Y (2012) *Manufacturing Automation: Metal Cutting Mechanics, Machine Tool Vibrations, and CNC Design*. Cambridge University Press

Publisher's Note Springer Nature remains neutral with regard to jurisdictional claims in published maps and institutional affiliations.

Springer Nature or its licensor (e.g. a society or other partner) holds exclusive rights to this article under a publishing agreement with the author(s) or other rightsholder(s); author self-archiving of the accepted manuscript version of this article is solely governed by the terms of such publishing agreement and applicable law.